atmosphere

MDPI

Article

Origin of the Fine Scale Tortuosity in Sparks and Lightning Channels

Vernon Cooray

Department of Engineering Sciences, Uppsala University, 751 21 Uppsala, Sweden; vernon.cooray@angstrom.uu.se

Received: 14 April 2018; Accepted: 21 May 2018; Published: 24 May 2018

Abstract: The physical reason for the small-scale tortuosity observed in sparks and lightning channels is unknown at present. In this paper, it is suggested that the small-scale tortuosity of the discharge channels is caused by the natural tendency for subsequent leader streamer bursts to avoid each other but at the same time to align as much as possible along the direction of the background electric field. This process will give rise to a discharge channel that re-orients in space during each streamer burst creating the small scale tortuosity.

Keywords: lightning; spark discharges; tortuosity; streamer bursts; leaders

1. Introduction

The tortuosity of spark and discharge channels has been observed since antiquity. The similarity of the tortuous nature of sparks and lightning channels is one reason that suggested to Benjamin Franklin that the basic physics underlying these two phenomena is the same. The first study that analysed the tortuous nature of the lightning channel qualitatively is probably that of Hill [1]. He analysed the nature of tortuosity and estimated that the average angle of tortuosity in lightning channels is about 17.3°. Since then, several studies have been conducted to analyse the tortuosity of lightning and spark channels both theoretically and experimentally [2–5].

One of the best recordings of the small scale tortuosity of the lightning channel with high resolution was obtained by Evans and Walker [4]. An Example from their study is shown in Figure 1. Note the fine scale tortuous structure of the channel. This is a photograph of a lightning channel taken from a distance of about 112 m. The lightning flash struck a tower of height 74 m located on a mountain. The details of the geometry pertinent to this photograph are shown in Figure 2. Since this strike took place on a tall tower, it is possible that the section of the lightning channel shown in the figure is created by the upward moving positive connecting leader.

The tortuosity of the lightning channel can affect the electromagnetic fields generated by return strokes, and this in turn may influence the disturbances caused by these electromagnetic fields in electrical systems [6–8]. Thus, the fine structure of the lightning channel is of interest, not only to physicists, but also to lightning protection engineers.

The exact reason for the appearance of small scale tortuosity in the lightning channel is unknown at present. Of course, the presence of branches also adds to the tortuosity of the lightning channel, but the fine scale tortuosity we are interested in here appears in channel sections without any branches. It has been suggested that the tortuosity of the lightning channel is caused by the diversion of the leader by the space charge pockets that exist in air between the cloud and the ground [9].

The large-scale tortuosity in the lightning channel could very well be due to space charge effects, but it is difficult to understand how the fine scale tortuosity observed experimentally could be explained by this mechanism. It is possible that the fine scale tortuosity associated with the discharge channels is different depending on whether the channel is created by a negative or a positive leader. This is the case

because the mechanism of propagation of negative leaders differs from that of the positive ones. In this paper, we will concentrate on the positive discharges because the mechanism of propagation of positive leaders is less complicated, and this mechanism is known better than that of negative discharges.

Here, we suggest that the fine scale tortuosity of the lightning channel sections and spark channels created by positive discharges is caused by the orientation of the leader streamer bursts in space to decrease the total energy associated with the leader streamer system. Of course, as we will discuss later, the same mechanism may be involved, at least partly, in the creation of channel tortuosity in negative discharges.

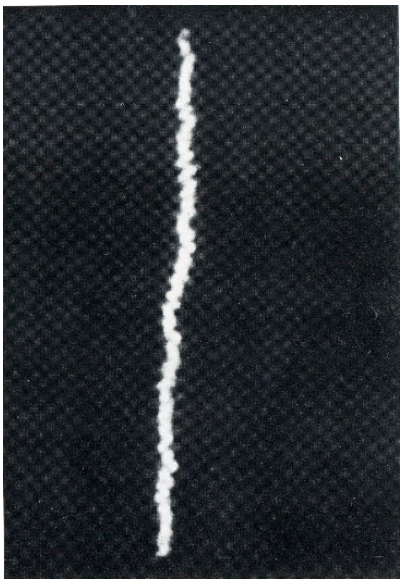

Figure 1. Fine scale tortuosity observed in the bottom 10 m or so of the lightning channel. Adapted from Reference [4].

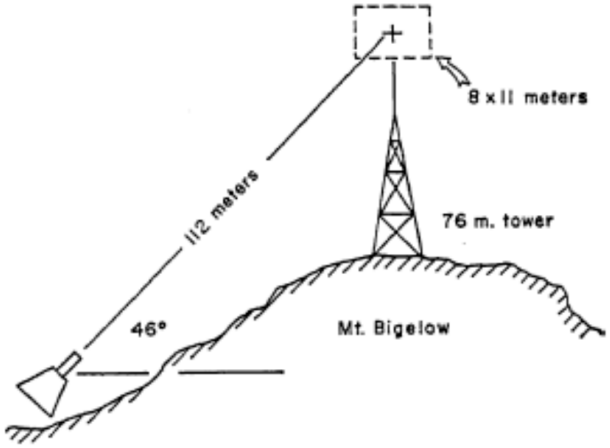

Figure 2. Geometry relevant to the acquisition of the photograph shown in Figure 1.

2. Mechanism of Propagation of Positive Leader Channels

Information gathered from long sparks shows that the positive leaders travel with the aid of streamer bursts generated from their tips. As the electric field increases and reaches a critical value at the point of origin of the positive leader, which could be the positive electrode in the laboratory setting or a lightning conductor or tower exposed to the electric field of the down-coming negative stepped leader, the point under consideration will give rise to a series of electron avalanches. In an increasing

electric field, these avalanches will be converted to streamers, and the result is a burst of positive streamers emanating from the tip of the point where the leader is initiated. Many of the streamers of this burst have their origin in a common channel called the streamer stem. The streamers travelling out from this common stem stop propagating when the background electric field decreases below a critical value necessary for their propagation. Each individual streamer is a cold discharge, and the current associated with it cannot heat the air sufficiently to make it conducting. However, the combined current of all streamers flowing through the common stem causes it to heat up, increasing the conductivity of the stem. When the temperature of the stem increases to about 1000–1500 K, the rate of negative ion destruction greatly increases, retarding the drop in conductivity. Furthermore, during the initial current flow through cold air, about 95% of the energy gained by electrons from the electric field is transferred to vibrations of nitrogen molecules [10,11]. The vibrational relaxation time decreases with increasing temperature. At around 1500–2500 K, the VT relaxation of nitrogen molecules is accelerated, and the energy stored in the vibrational states of the molecules transfers to the translational energy, thus raising the temperature. The increase in the temperature causes the gas to expand, making the E/n (E is the electric field and n is the gas density) ratio to increase, which leads to an increase in ionisation and electron production. Thus, the current will be concentrated into a thin channel, and this in turn produces more heating and accelerates the ionisation. Through this process, the stem will be transformed into a hot and conducting channel called the leader.

Owing to the high conductivity of the leader channel, the voltage of the object that gave rise to the leader will be transferred to the head of the leader channel, resulting in a high electric field there. The production of streamer discharges now takes place from the head of the common stem (or the newly created leader). As before, these streamers will be attached to a common stem which, with the aid of cumulative streamer currents, gradually transforms itself to a conducting channel, making it a part of the leader channel. The process is repeated again and again, and each time it happens, the leader length is extended by a certain amount. Indeed, the streamer system located in front of the leader is the source of current which heats the air and makes possible the elongation of the leader. As the leader progresses forward through the space originally traversed by streamers, the charge of the latter forms a space charge or corona sheath around the leader channel.

In the analysis of the propagation of the leader, it is usually assumed that each streamer burst is generated in the same direction as the previous one [12,13]. However, this assumption completely neglects the fact that the region ahead of the tip of the last section of the leader channel is filled with the positive charge of the last streamer burst, and creating another streamer burst with the same polarity of charge through the same region is energetically unfavourable. It is reasonable to assume that the new streamer burst completely avoids the previous streamer burst and generates streamers in a new direction that does not overlap with the streamers of the previous burst. However, there are two conditions that the direction of the new streamer burst has to satisfy. As mentioned previously, the new streamer burst should avoid the positive charge of the previous streamer burst. Second, the direction of the streamer burst should be such that it will minimize the energy of the system. In other words, while avoiding the location of the previous streamer burst, the new streamer burst should take place in a direction so that the leader is elongated in the general direction of the background electric field. Location and extension of streamer bursts based on these two criteria generates a leader channel which continuously re-orients itself after each streamer burst.

The simulation of the inception and propagation of the leader channel is conducted in a manner essentially similar to that used in the Self consistent Leader Inception and propagation Model SLIM [14] with a slight modification. As in SLIM, the first streamer burst that will give rise to the first leader segment is assumed to be oriented vertically. The length of the streamer burst and its charge is calculated using the procedure documented in [14]. The next streamer burst is assumed to take place in any direction (but not vertical) that will minimize the energy of the streamer leader system. The optimal direction of the second streamer burst is obtained by selecting all possible orientations of the second streamer burst and calculating, in each case, the energy associated with the system (i.e., due

to charges on the tower, the charges of the previous streamer bursts, and the background electric field). The direction that minimizes the energy is selected as the optimal direction. In calculating the energy of the system, the charge associated with each streamer burst is assumed to be distributed uniformly along the central axis of the streamer burst. The same procedure is followed in obtaining the direction of successive streamer bursts.

3. The Model

As observed in the experiments and described in the last section, a positive leader starts from an object where the electric field at its tip is near the breakdown electric field. In the simulation, we consider a lightning rod or a tower located in a background electric field. The electric field is increased to a level sufficient to the initiation of a positive leader. The process of initiation of a leader and its subsequent propagation with the aid of streamer bursts are considered as follows.

(1) When the background electric field is high enough, electrical avalanches will be initiated from the tip of the object under consideration, and if the background electric field reaches a certain threshold, which depends on the geometry of the object under consideration, the avalanches will be converted to streamers. The first step in the simulation is to investigate whether the selected background electric field is strong enough to give rise to a streamer burst. If the selected value of the electric field is not large enough to generate streamers, it is increased until the streamers are incepted from the tip of the object under consideration.

(2) The first streamer burst takes place along the direction of the background electric field, and in this case, it takes place along a vertical line. The experimental data show that positive streamers require a background electric field of about 0.5×10^6 V/m for stable propagation [15]. The length of the streamer burst is calculated by plotting both the background potential and the streamer potential as a function of distance from the tip of the lightning conductor. The streamer zone is assumed to maintain a constant potential gradient E_s, and in the distance–voltage diagram, the potential along the streamer region is represented by a straight line (see Figure 3). The point of intersection of these two potentials gives the length of the streamer region. In the analysis to follow, it is assumed that $E_s = 0.5 \times 10^6$ V/m [15].

(3) The charge in the positive streamer burst generated from the space leader is calculated following the procedure outlined in [14]. The charge associated with these streamer bursts is calculated using the same distance–voltage diagram used in the previous step. The procedure is illustrated in Figure 3. If the area between the two curves representing the streamer potential and the background potential up to the point where they cross is A (see Figure 3), the charge in the streamer zone is given by

$$Q_{ns} \approx K_Q A \tag{1}$$

In the above equation, K_Q is a geometrical factor. Becerra and Cooray [13,14] estimated its value to be about 3.5×10^{-11} C/V m. For the energy calculations to follow, it is necessary to know the charge distribution inside the streamer burst. In the calculations to follow, it is assumed that the charge of each streamer burst is concentrated along the central line, and this charge is distributed uniformly along this line. This is the only simplifying assumption made in the study, and this assumption is necessary to evaluate the energy of the system at any given time of the development of the leader channel. The information concerning the magnitude of the charge and its distribution for each streamer burst is stored in the program so that, in the energy calculation, the contributions from the charge distributions associated with all the previous streamer bursts could be included.

(4) The currents associated with the streamers convert their common stem into a hot channel, and it becomes part of the leader channel. Following the procedure introduced in [14], the extension of the leader during each streamer burst is assumed to be $|Q_{ns}|/q_l$, where q_l is the charge necessary to thermalize a unit length of the leader channel. Based on the theory of Gallimberti [10], it is assumed to be equal to 60 μC/m.

(5) Once the location of the new tip of the leader is estimated as described in the previous step, the simulation is ready to calculate the second burst of the streamers that will be generated from the new leader tip. The direction of the second burst of the streamers is estimated by minimizing the electrostatic energy associated with the charges in the streamer bursts and the background electric field. This is done as follows. Let us define angles θ and φ as the polar and azimuthal angles with respect to the axis of the previous streamer burst. These angles can take any value between 0 to π and 0 to 2π, respectively. For any given direction pertinent to a given set of θ and φ, the length on the streamer burst and the charge associated with it is estimated. From this, the energy associated with the system is calculated. The same procedure is done by changing the two angles over the given range in intervals of 1°. From this calculation, the direction that minimizes the energy is obtained, and this is considered to be the direction of the new streamer burst. Note that, in the case of the second burst, the energy depends only on the angle θ and not on φ. This is the case because the direction of the first streamer burst is along the vertical axis. In this case, the program selects a value for the angle φ at random. Figure 4 illustrates the scenario of the process described above.

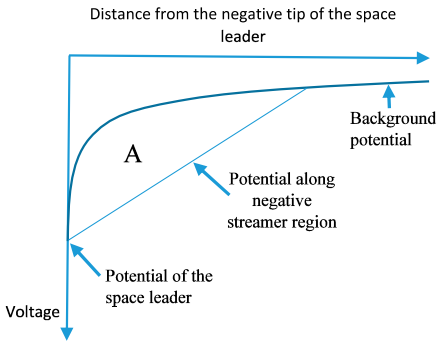

Figure 3. Distance–voltage diagram that illustrates how the charge associated with a streamer burst is obtained. The area between the two curves representing the background potential and the streamer potential is marked A.

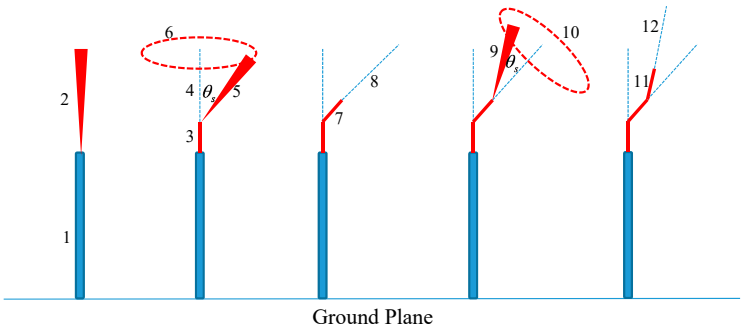

Figure 4. The first streamer burst (marked 2) from the lightning conductor (marked 1) takes place in a vertical direction (marked 4). This streamer burst gives rise to the first leader section (marked 3). The direction of the second streamer burst (marked 5) is estimated by considering all the possible directions around the direction of the first streamer burst (i.e., all values of θ and φ) and finding the direction that minimizes the electrostatic energy of the system. The circle marked 6 shows the location of different directions for a given value of φ. The second streamer burst gives rise to a new leader section (marked 7). The direction of the third streamer burst (marked 9) is obtained by going around the direction of the second streamer burst (marked 8) and finding the direction that minimizes the electrostatic energy. The circle marked 10 shows the location of different directions for a given value of φ measured with respect to the direction of the second streamer burst. The third streamer burst gives rise to the third leader section (marked 11) which is directed along the line marked 12. The process is continued to obtain the full geometry of the leader channel.

4. Results and Discussion

The analysis is conducted by using an earthed rod exposed to a uniform background electric field. In the analysis, the length of the rod is changed from 25 m to 100 m, and the radius of the rod is changed from 1 cm to 10 cm. The background electric field is selected always in such a way that a continuous propagating leader is established from the rod. These considerations led to background electric fields in the range 3.5 kV/m to 30 kV/m. The polarity of the electric field is such that the upward moving leader has the positive polarity. In the calculations, we have documented the x, y and z (vertical) coordinates of the leader sections, and for this reason, for any given configuration, one can plot the x–z and y–z projections.

The results of our simulations are shown in Figures 5–8. In each figure, the height of the conductor, its radius, and the background electric field is given. Figure 5 shows the geometry of the positive leader for a 100 m long rod with a 5 cm radius. The background electric field is 7.5 kV/m. Observe the fine structure of the leader geometry. This variation is caused by the rotation of the streamer bursts away from the previous one. The result obtained for a 25 m rod with a 1 cm radius is shown in Figure 6. The background field pertinent to this case is 15 kV/m. Figures 7 and 8 depict similar data but for background electric fields of 20 kV/m and 30 kV/m, respectively. Note that, irrespective of the rod length or the background electric field, the displacement of the streamer bursts from each other will give rise to the fine scale tortuosity of the channel. The scale of the tortuosity that is shown in the diagrams takes place for leader segments on the order of a few centimetres. This scale changes with an increase in the electric field because the leader segments created by each streamer burst increases with an increasing electric field. For example, Figure 9 depicts the fine structure associated with the leader segments of a 25 m long rod with a 1 cm radius for three different background electric fields. Observe how the length of the leader segments increases with an increasing background electric field. This increase is caused by the large charge associated with the streamer bursts and, hence, the length of the newly created leader segments as the background electric field increases.

Due to the repulsion between the charges associated with streamer bursts, each new streamer burst finds the best direction that minimizes the energy of the system while advantageously aligning along the background electric field in minimizing this energy. In a three-dimensional space, this gives rise to a rotation of the propagating leader channel. This is illustrated in a 3-D diagram given in Figure 10.

Observe the tortuous nature of the leader channel and its similarity to the fine structure captured in the photographs of the lightning channel by Evans and Walker [4]. Recall that we are simulating the upward moving positive leaders. In the case of Evans and Walker [4], the photograph corresponds to the bottom 10 m or so of a lightning flash that struck a 74 m tall tower located on a mountain. It is thus reasonable to assume that this portion of the lightning channel is created by an upward moving positive connecting leader.

It is important to point out that the current flowing along the leader channel can exert magnetic forces on the tortuous channel, and the direction of these magnetic forces makes the channel straighter. This process is not included in the present paper. However, it is possible that the mechanical displacement of the channel due to magnetic forces may take a longer time than the duration of the lightning flash. This is an interesting topic that needs investigation.

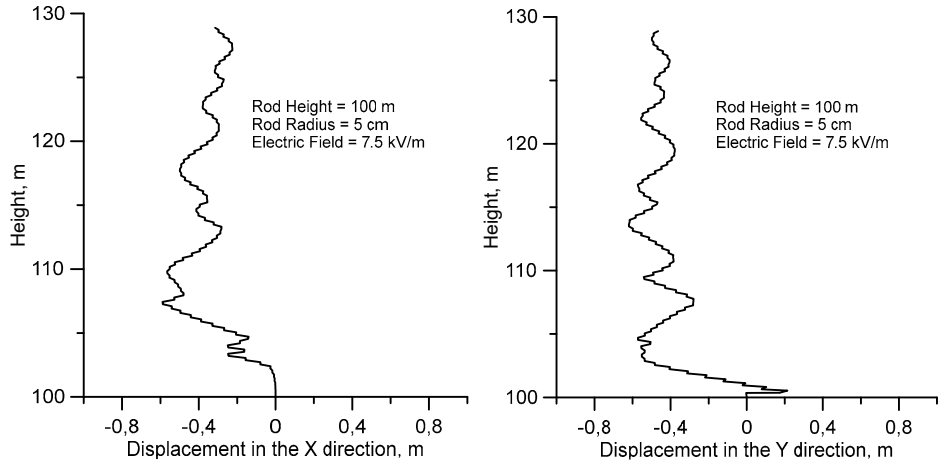

Figure 5. The *x*–*z* and the *y*–*z* projections of the leader channel generated by a 100 m long rod of 5 cm radius located in a background electric field of 7.5 kV/m.

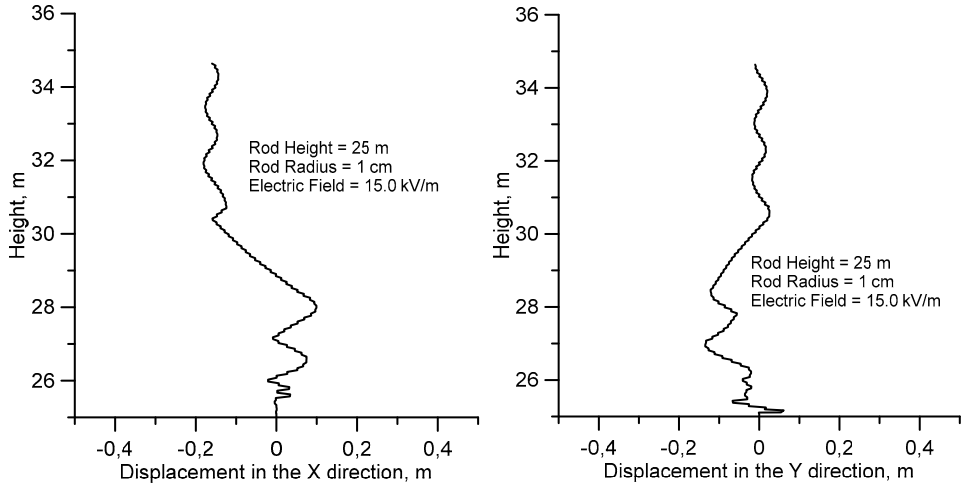

Figure 6. The *x*–*z* and the *y*–*z* projections of the leader channel generated by a 25 m long rod of 1 cm radius located in a background electric field of 15 kV/m.

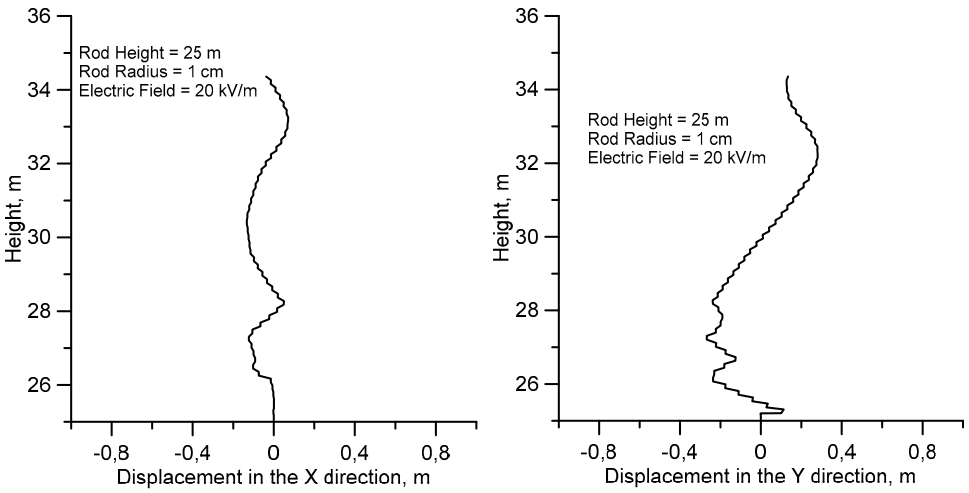

Figure 7. The *x*–*z* and the *y*–*z* projections of the leader channel generated by a 25 m long rod of 1 cm radius located in a background electric field of 20 kV/m.

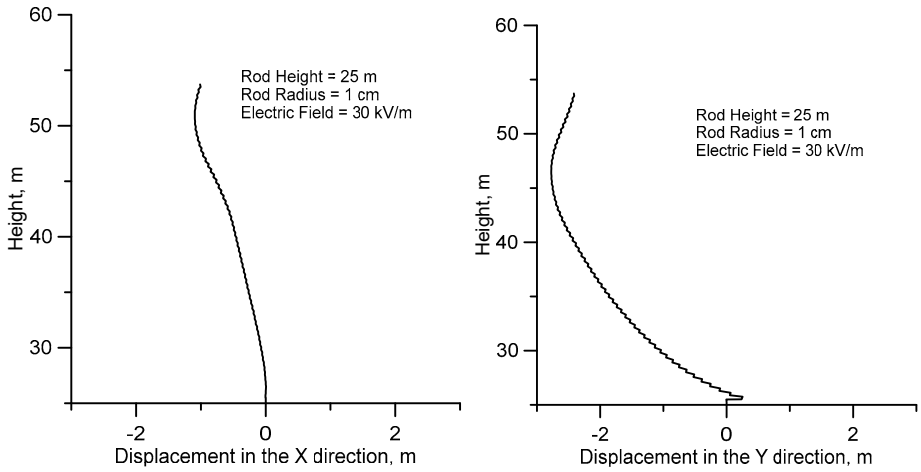

Figure 8. The *x*–*z* and the *y*–*z* projections of the leader channel generated by a 25 m long rod of 1 cm radius located in a background electric field of 30 kV/m.

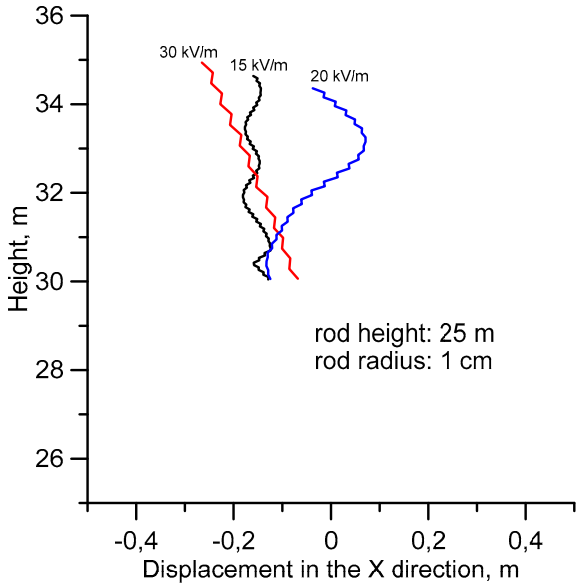

Figure 9. The *x*–*z* projection of the leader channel segments generated by a 25 m long rod of 1 cm radius located in three background electric fields, namely, 30 kV/m, 20 kV/m, and 15 kV/m.

One interesting question that we can raise at this point is the following: Can negative leaders also generate fine structure similar to that predicted to exist in positive leaders? First, one has to note that positive leaders not only are present in isolation, but also are involved in the creation of negative leader channels. A major part of the steps of negative leaders are actually forged by positive space leaders that begin at the extremity of the streamer region of the negative leader and propagate towards the tip of the negative leader [16]. It is difficult to speculate whether reorientation of the streamer bursts will also take place in the case of space leaders propagating towards the leader tip. The space leaders are moving in a very high electric field, and this may compensate somewhat for the energy necessary in the overlapping of successive streamer bursts of the same polarity.

The main point illustrated in this paper is the possible rotation of the streamer bursts from each other to minimize the electrostatic energy associated with the charges deposited by streamers. Actually, laboratory spark experiments combined with high speed photography can indeed be used to study the spatial evolution of the streamer bursts in space and confirm whether they will change direction in space as they move forward.

The leader model presented here could be used to study the nature of electromagnetic fields generated by tortuous channels and investigate whether the tortuous channels are responsible for part of the High Frequency (HF) and Very High Frequency (VHF) generated by lightning discharge processes such as compact cloud discharges [17–20].

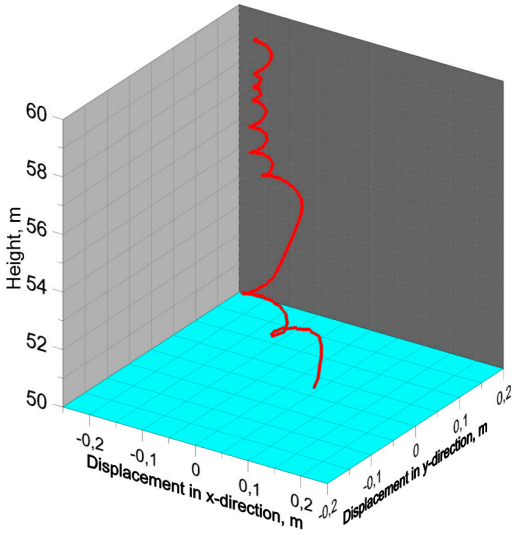

Figure 10. A 3-D diagram of the leader channel generated by a 50 m long rod of 1 cm radius located in a background electric field of 7.0 kV/m. Note the rotation of the leader channel in space.

5. Conclusions

In this paper, we suggest that the fine structure that has been photographically documented in the lightning channels is created by the reorientation of the successive streamer bursts in leaders to minimize the electrostatic energy of the streamer–leader system.

Conflicts of Interest: The authors declare no conflict of interest.

References

1. Hill, R.D. Analysis of irregular paths of lightning channels. *J. Geophys. Res.* **1968**, *73*. [CrossRef]
2. Idone, V.P.; Orville, R.E. Channel tortuosity variation in Florida triggered lightning. *J. Geophys. Res. Lett.* **1988**, *15*, 645–648. [CrossRef]
3. Hill, R.D. Tortuosity of lightning. *Atmos. Res.* **1988**, *22*, 217–233. [CrossRef]
4. Evans, W.H.; Walker, R.L. High speed photographs of lightning at close range. *J. Geophys. Res.* **1963**, *68*, 4455–4461. [CrossRef]
5. Mousa, A. Failure of the collection volume method and attempts of the ESE lightning rod industry to resurrect it. *J. Light. Res.* **2012**, *4*, 118–128. [CrossRef]
6. Cooray, V.; Orville, R. The effects of variation of current amplitude, current risetime and return stroke velocity along the return stroke channel on the electromagnetic fields generated by return strokes. *J. Geophys. Res.* **1990**, *95*, 18617–18630. [CrossRef]
7. Cooray, V.; De la Rosa, F. Shapes and amplitudes of the initial peaks of lightning-induced voltage in power lines over finitely conducting earth: Theory and comparison with experiment. *IEEE Trans. Antenn. Propag.* **1986**, *34*, 88–92. [CrossRef]
8. Nucci, C.A.; Rachidi, F.; Ianoz, M.V.; Mazzetti, C. Influence of a lossy ground on lightning induced voltages on overhead lines. *IEEE Trans. Electromagn. C* **1993**, *35*, 75–86. [CrossRef]
9. Schonland, B.F.J.; Allibone, T.E. Branching of lightning. *Nature* **1931**, *128*, 794–795. [CrossRef]
10. Gallimberti, I. The mechanism of the long spark formation. *J. Phys. Colloq.* **1979**, *40*, 193–250. [CrossRef]
11. Bazelyan, E.M.; Raizer, Y.P. *Spark Discharge*; CRC Press: Boca Raton, FL, USA, 1997.

12. Goelian, N.; Lalande, P.; Bacchiega, G.L.; Gazzani, A.; Gallimberti, I. A simplified model for the simulation of positive-spark development in long air gaps. *Appl. Phys.* **1997**, *30*, 2441–2452. [CrossRef]
13. Beccerra, M.; Cooray, V. A simplified physical model to determine the lightning upward connecting leader inception. *IEEE Trans. Power Deliv.* **2006**, *21*, 897–908. [CrossRef]
14. Becerra, M.; Cooray, V. A self-consistent upward leader propagation model. *J. Phys. D Appl. Phys.* **2016**, *39*, 16. [CrossRef]
15. Les Renardières Group. Research on long gap discharges at Les Renardières. *Electra* **1972**, *23*, 53–157.
16. Cooray, V.; Arevalo, L. Modeling the Stepping Process of Negative Lightning Stepped Leaders. *Atmosphere* **2017**, *8*, 245. [CrossRef]
17. LeVine, D.M. Sources of strongest RF radiation from lightning. *J. Geophys. Res.* **1980**, *85*, 4091–4095. [CrossRef]
18. Willett, J.C.; Bailey, J.C.; Krider, E.P. A class of unusual lightning electric field waveforms with very strong HF radiation. *J. Geophys. Res.* **1989**, *94*, 16255–16267. [CrossRef]
19. Nag, A.; Rakov, V.A.; Tsalikis, D.; Cramer, J.A. On phenomenology of compact intracloud lightning discharges. *J. Geophys. Res.* **2010**, *115*, D14115. [CrossRef]
20. Ahmad, N.A.; Fernando, M.; Bahaudin, Z.A.; Cooray, V.; Ahmad, H.; Malek, Z.A. Characteristics of narrow bipolar pulses observed in Malaysia. *J. Atmos. Sol. Terr. Phys.* **2010**, *72*, 534–540. [CrossRef]